

Nonlocality in the density-functional description of bonding in Li₂, N₂, O₂, and F₂

Frank W. Kutzler

Department of Chemistry, Tennessee Technological University, Cookeville, Tennessee 38505

G. S. Painter

Metals and Ceramics Division, Oak Ridge National Laboratory, Oak Ridge, Tennessee 37831

(Received 21 September 1987)

The fully self-consistent implementation of the nonlocal-density functional of Langreth and Mehl has been used in conjunction with the augmented Gaussian method to calculate the potential-energy curves and dissociation energies of N₂, Li₂, O₂, and F₂. The nonlocal functional gives ground-state potential-energy curves in very good agreement with experiment. We compare these nonlocal results with other local-density calculations, and examine the effect of nonlocal-potential self-consistency on the dissociation energy.

I. INTRODUCTION

The local-spin-density approximation (LSDA), a specialization of the general density-functional theory originated by Hohenberg, Kohn, and Sham,^{1,2} has been used to calculate the electronic ground-state properties of numerous atoms and molecules. Most undertakings have been surprisingly successful—trends in electron densities, ionization and binding energies, and molecular geometries are well reproduced and quantitative accuracy in geometries is usually to within 1–2%.³ The lack of corresponding accuracy in binding energies remains a major shortcoming of the LSDA.

The fundamental local-density approximation is that the exchange-correlation energy of a system of interacting electrons can be calculated from an integral involving the exchange-correlation energy density, ϵ_{xc} :

$$E_{xc} = \int d\mathbf{r} n(\mathbf{r}) \epsilon_{xc}(n(\mathbf{r})). \quad (1)$$

The exchange-correlation potential v_{xc} is computed from the functional derivative of the energy density

$$v_{xc} = \frac{\partial}{\partial n(\mathbf{r})} n(\mathbf{r}) \epsilon_{xc}(n(\mathbf{r})). \quad (2)$$

These local functionals are approximated as the exchange-correlation energy density and potential of a homogeneous electron gas with the charge density $n(\mathbf{r})$.

Two basic errors are entailed in the LSDA. First, the exchange-correlation energy and potential of the interacting (correlating) electron gas are imprecisely known. The more recent LSDA functionals are parametrizations^{4,5} of electron gas results calculated by the random-phase approximation (RPA) and by Monte Carlo methods. Both approximate Coulomb correlation effects.

The second error is that the charge densities of atoms and molecules are not uniform, and the exact exchange interaction (given by Hartree-Fock theory) is not local. Recent progress toward removing this error has come from gradient or *nonlocal* functionals,^{6–8} which depend

on both the charge density and the gradient of the charge density. These functionals are nonlocal in the sense described by Parr,⁹ though the functional still depends on the properties of the charge density only within an infinitesimal volume element.

This paper reports results from a study assessing the effects of a full implementation of the Langreth-Mehl (LM) nonlocal-density functional^{7,8} on the dissociation curves for several diatomic molecules.

II. METHOD

The LM nonlocal exchange-correlation energy of an inhomogeneous electronic charge distribution is given by

$$E_{xc}[n] = E_{xc}^{local} + \int d\mathbf{r} n(\mathbf{r}) \epsilon_{nl}^{xc}[n(\mathbf{r})],$$

where $\epsilon_{nl}^{xc}[n(\mathbf{r})]$ is the energy density per particle;

$$\epsilon_{nl}^{xc} = a \int d\mathbf{r} \left[\frac{-7}{9 \times 2^{1/3}} \left[\frac{|\nabla n_+|^2}{n_+^{4/3}} + \frac{|\nabla n_-|^2}{n_-^{4/3}} \right] + \frac{2}{d} e^{-F} \frac{|\nabla n|^2}{n^{4/3}} \right], \quad (3)$$

where

$$F = b \frac{|\nabla n|}{n^{7/6}},$$

$$d = 2^{-1/2} [(1+\zeta)^{5/3} - (1-\zeta)^{5/3}]^{1/2},$$

$$\zeta = (n_+ - n_-) / n,$$

$$n = n_+ + n_-.$$

The constants a and b are (in atomic units)

$$a = \frac{1}{2} \{ \pi / [8(3\pi^2)^{4/3}] \} = 2.1435 \times 10^{-3},$$

$$b = (9\pi)^{1/6} f = 1.745 f,$$

and f is an adjustable parameter which defines a cutoff wave vector used in the integration over the wave-vector decomposition of the nonlocal contribution to the corre-

lation energy.^{7,8} (The derivation and discussion of these equations appear in Refs. 7 and 8.) The optimal value for f is weakly system dependent and ranges between 0.13 for surfaces and 0.17 for atoms and molecules. Un-

less otherwise states, we have adopted $f=0.15$ for the calculations reported here.

The exchange-correlation potential v_{xc} is obtained via Eq. (2),

$$v_{\pm}^{xc}[n] = v_{\pm,local}^{xc} + \frac{a}{n^{1/3}} \left\{ \frac{-7}{9 \times 2^{1/3}} \left[\frac{4|\nabla n_{\pm}|^2}{3n_{\pm}^2} - \frac{2\nabla^2 n_{\pm}}{n_{\pm}} \right] \left(\frac{n_{\pm}}{n} \right)^{-1/3} - \frac{2}{d} e^{-F} \left[\frac{(2-F)\nabla^2 n}{n} \left[\frac{4}{3} - \frac{11F}{3} + \frac{7F^2}{6} \right] \frac{|\nabla n|^2}{n^2} + \frac{F(F-3)(\nabla n \cdot \nabla)(|\nabla n|)}{n|\nabla n|} - \frac{5n^{1/3}(n_{\pm}^{2/3} - n_{\mp}^{2/3})}{6d^2 n^4} \nabla n \cdot [2^{2/3}(1-F)n_{\mp} \nabla n - 2^{2/3}(2-F)n \nabla n_{\mp}] \right] \right\}. \quad (4)$$

The nonlocal portion of the potential, v_{xc} , diverges at small $n(\mathbf{r})$ (large \mathbf{r}), and Langreth and Mehl suggested multiplying both $v_{\pm,nl}^{xc}$ and ϵ_{nl}^{xc} by a suppression factor⁷

$$c = \exp(-h|\nabla n|^2 n^{-8/3}), \quad (5)$$

where h was chosen to be 0.0001. This topic will be addressed in more detail below.

These nonlocal functionals are combined with one of the local exchange-correlation parametrizations of the RPA electron gas calculation. We have chosen the Vosko-Wilk-Nusair fit of RPA data (VWN RPA).⁵

Equations (3) and (4) were incorporated into the augmented Gaussian orbital method of Painter and Averill.¹⁰ In the version used in this study, the basis was divided into two sets of atom-centered Gaussians.¹¹ One set of Gaussians has large exponential constants and, to within a small tolerance, is nonzero only within a predefined sphere centered on the atom site. These functions describe the core region of the basis orbitals. The other set has smaller exponential constants and extends beyond the atomic spheres; this set forms the exclusive representation of the tails of the valence orbitals. This dual basis set allows independent optimization of the numerical integrations over the core and valence regions. The numerical integration involved in evaluation of the electron-electron matrix elements was done on a spherical point mesh around each atom (for the core and valence sets) and on a global prolate spheroidal mesh (for the valence set only). The all-Gaussian basis is par-

ticularly advantageous in the present context because the charge-density gradients can be computed analytically.

Both local and nonlocal potentials were iterated to self-consistency, except where otherwise noted. The size of the basis sets for Li, N, and the dimers are noted in Tables I and II. The basis for O was (10s, 6p) and for F the basis was (12s, 6p).

III. RESULTS

A. Atomic tests

Gaussian functions poorly represent the cusp in the s -orbital charge density at the nucleus, and the gradient representation is even poorer. Hence we sought to establish that an all-Gaussian basis of moderate size was suitable for gradient functionals. Table I is a comparison between atomic energies taken from Langreth and Mehl,⁷ who used a numerical method, and our Gaussian orbital calculations. When we use the von Barth-Hedin (vBH) RPA parametrization,⁶ the total energies agree to within 0.005 hartrees. Table I also shows the minor differences that occur when the VWN RPA (Ref. 7) is used rather than vBH for the local portion. The basis sets used in our calculations for the atoms are also noted in Table I. We conclude that with a sufficient basis, the incorrect behavior near the nucleus has a negligible effect on the total energy.

TABLE I. Comparison of atomic total energies calculated numerically (Ref. 7) and from a Gaussian basis set (in hartrees). Calculations done with $f=0.15$ (see text).

Atom	Basis size	LM ^a	Present (vBH local)	Present (VWN local)
He	(10s)	-2.90	-2.8980	-2.8998
Li	(8s)	-7.46	-7.4570	-7.4538
Be	(13s)	-14.60 ₅	-14.6030	-14.6088
N	(10s, 6p)	-54.44 ₅	-55.4450	-54.4629
Ne	(14s, 8p)	-128.68	-128.6758	-128.7000

^aThe values from Refs. 7 and 8 are reported in rydbergs. We have divided by 2 and when this division resulted in a remainder, a subscript "5" is recorded.

TABLE II. Comparison of calculated and experimental vibrational frequencies (in cm^{-1}).

Dimer	Basis	Expt.	Fitted expt. ^a	LM	VWN (local)
Li_2	[8s3p1d/5s3p1d]	351	357	364	356
N_2	[10s6p1d/5s4p1d]	2358	2377	2409	2430
O_2	[10s6p1d/5s4p1d]	1580	1611	1624	1628
F_2	[12s6p1d/5s4p1d]	892	994	1067	1091

^aFrom RKR data (Ref. 12) for Li_2 , N_2 , and O_2 , and from Hulburt-Hirschfelder (Ref. 14) for F_2 , as described in text.

B. Dissociation curves

A variety of treatments for N_2 have appeared in the literature. In Fig. 1, we compare the experimental N_2 binding-energy curves to curves from other calculations. In order to better compare the shapes of the curves, we have adjusted each curve along the energy axis to a common reference energy. The coincidence of the minima shows that all curves have nearly the same equilibrium separation. It is also apparent that the shape of the LM exchange-correlation curve, denoted by diamond markers, is in excellent agreement with the Rydberg-Klein-Rees¹² experimental (EXPT) curve (the solid line). By comparison the Hartree-Fock (HF) (dashed) curve rises too steeply at large R . This is expected for Hartree-Fock, which predicts the wrong dissociation limit. Conversely, the LM exchange-only (dash-dotted) curve

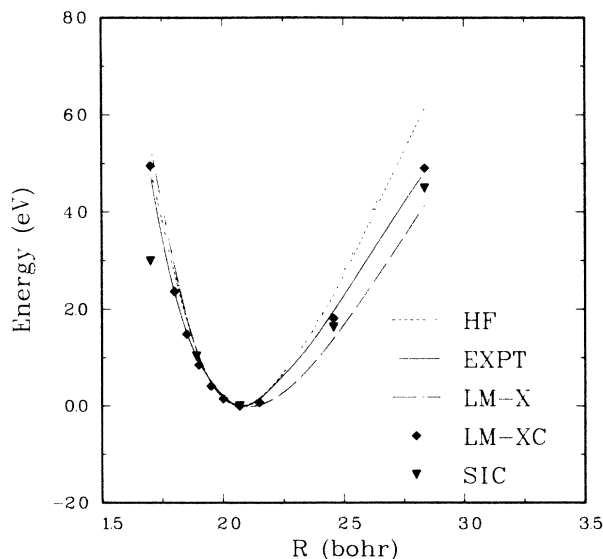


FIG. 1. Potential-energy curves for the nitrogen molecule calculated from several exchange-correlation functionals. The solid line (EXPT) is the Rydberg-Klein-Rees experimental binding curve (Ref. 12). To better compare the shapes, all curves have been shifted along the energy axis to a common zero. The HF curve (dotted line) and the self-interaction-corrected results (SIC, triangles) are taken from Pederson *et al.* (Ref. 13). The Langreth-Mehl nonlocal exchange-only functional (LM-XC) gives the dot-dashed line, and results using the LM nonlocal exchange and correlation functional (LM-XC) are shown by diamond markers.

(LM-X) rises too slowly. The comparison between HF and LM exchange-only curves (by definition, the exact density-functional exchange energy is identical to the Hartree-Fock exchange energy) shows the amount of error in the R dependence of the LM exchange, although exchange plus correlation produces a curve with nearly the same R dependence as experiment. Also noted (by triangles) is the self-interaction-corrected (SIC) potential curve of Pederson *et al.*¹³ The SIC results are in reasonably good agreement with experiment for large R , but show a softer curve for compressed bond lengths than experimentally observed. The VWN local potential-energy curve is not shown because it is very nearly the same as the LM-XC curve. Thus nonlocality has, in fact, little effect in changing the *shape* of the N_2 binding curve, but does improve the *magnitude* of the dissociation energy, as discussed below. Although not shown, the curves for Li_2 , O_2 , and F_2 are also in good agreement with their experimental curves.

We feel a comparison of theoretical versus experimental curves over a wide range of geometries offers the best test of a calculation. Nevertheless, a concise, quantitative comparison is possible by extracting the equilibrium separation R_e and the vibrational frequency ω_e from the theoretical curve.

Unfortunately, procedures for obtaining ω_e are sensitive to the separation distances chosen for curve fitting. To filter out fitting error, we have fit both theoretical *and* experimental curves to a third-order polynomial, using the same atom separations in both cases. For Li_2 , N_2 , and O_2 , we chose the equilibrium separations plus the Rydberg-Klein-Rees¹² turning points of the lowest three vibrational levels. For F_2 we chose seven evenly spaced geometries ranging from 2.368 to 2.968 a.u. The experimental F_2 values were calculated using the Hulburt-Hirschfelder curve¹⁴ calculated from experimental constants.¹⁵

The results are tabulated in Table II. The error inherent in the curve fitting is shown by the difference between the experimental and fitted experimental values. The close (1–2%) agreement between the fitted experimental and the fitted theoretical curves for Li_2 , N_2 , and O_2 demonstrates the accuracy of the shape of the theoretical curve. Moreover, ω_e is at least slightly better in the nonlocal than the local calculation, with the exception of Li_2 , where the local results may be fortuitously good. The calculated ω_e for F_2 is not as good as for the other dimers, but here, too, nonlocality improves upon the LSDA.

TABLE III. Results of binding-energy calculations for N_2 . Comparison of the effects of self-consistency, of the choice of f , and of the suppression of ϵ_{nl}^{xc} at large r . Total energies are in hartrees, binding energies in eV. Non-self-consistent calculations were done with an exchange-only $X\alpha$ ($\alpha = \frac{2}{3}$) self-consistent density.

f	Self-consistent?	Suppressed ϵ_{nl}^{xc} ?	Total energies		Binding energy
			N_2	N	
0.15	No	No	-109.292 43	-54.460 41	-10.11
0.15	Yes	No	-109.297 18	-54.462 89	-10.11
$\frac{1}{6}$	No	No	-109.337 83	-54.484 00	-10.06
$\frac{1}{6}$	Yes	No	-109.342 71	-54.486 56	-10.06
0.15	No	Yes	-109.286 45	-54.453 26	-10.34
0.15	Yes	Yes	-109.291 14	-54.455 79	-10.33

C. Binding energies

Binding energies calculated within the LSDA for O_2 , N_2 , and F_2 differ considerably with the experimental values. Most LSDA calculations, though, overbind dimers which form p bonds.¹⁶ Calculations going beyond the LSDA have done better. For example, Pederson *et al.*¹³ report an unusually close binding energy of -9.94 eV calculated from a SIC N_2 total energy and a SIC atomic energy by Harrison,¹⁷ and Becke has obtained good results incorporating a nonlocal semiempirical functional into a numerical method designed especially for dimers.¹⁸

There are several choices one must make when calculating a LM binding energy. We wanted to explore the sensitivity of the binding energy to three of the choices: (1) the self-consistency of the nonlocal potential, (2) the choice of the cutoff parameter f , and (3) the suppression of the divergent nonlocal potential. We focused on the N_2 binding energy to examine these effects. All calculations were done at the experimental bond length (2.074 bohrs, 1.098 Å). (The total molecular energies of the experimental and calculated bond lengths are virtually identical.)

We tested the importance of a self-consistent nonlocal potential by computing the binding energy with a self-consistent $X\alpha$ exchange-only ($\alpha = \frac{2}{3}$) density. This binding energy is then compared to the value for a totally self-consistent calculation. Comparing the first and second rows (or third and fourth, or fifth and sixth) of Table III, one can see that self-consistency lowers the total energy by 0.13 eV (in N_2), but that a corresponding drop in the energy of the atom leaves the dissociation energy unaffected. Nonlocal changes in the charge density have little effect on the binding energy of N_2 .

The optimum value of f changes for different systems,⁷ so we have compared the binding energies of N_2

using two reasonable molecular values, $f = 0.15$ and $f = \frac{1}{6}$. The total energies are moderately affected by changing f (~ 1.2 eV in N_2), but, as in the case of self-consistency, a compensating change in the energy of the atom results in only a small change in the binding energy.

The divergence of v_{nl}^{xc} at large r was mentioned above. In the earlier LM paper,⁷ both ϵ_{nl}^{xc} and v_{nl}^{xc} were multiplied by the factor shown in Eq. (5). In the more recent spin-polarized version by Hu and Langreth,⁸ this suppression was applied to v_{nl}^{xc} , but not to ϵ_{nl}^{xc} .

To test the effect of the suppression on the binding energy, we calculated binding energies both with and without suppression of ϵ_{nl}^{xc} . Spin-dependent terms were suppressed by an expression similar to Eq. (5), except that n_+ or n_- was used rather than the total density. The parameter h was set at 0.0001, as in Ref. 7.

The fourth and sixth rows of Table III show that the total energies change only slightly with suppression (~ 0.006 hartrees out of ~ 109 for N_2). But the binding energy, which is sensitive to changes that affect molecules and atoms differently, increases by ~ 0.23 eV. This is a modest increase, but it is larger than differences due either to the choice of f or to self-consistency. An increase in binding energy with ϵ_{nl}^{xc} suppression also occurs for F_2 and Li_2 .

The binding energies of the other dimers were calculated using $f = 0.15$, a fully self-consistent potential, and without suppression of ϵ_{nl}^{xc} . The results are shown in Table IV. In all four cases, the nonlocal functional lowers the binding energies, and except for Li_2 (where local theory is very close) this is an improvement. The binding energies of F_2 and O_2 can be further improved by removing the spherical averaging over the partially occupied atomic p shells. However, we have used spherical atomic charge densities for the results in Table IV so that we may show only the effects of the nonlocal func-

TABLE IV. Comparison of binding energies (in eV) and equilibrium separation (in a.u.).

Dimer	Binding energy			Experiment	R_e	
	Experiment	LM	VWN		LM	VWN
Li_2	1.03	0.60	1.04	5.05	5.22	5.16
N_2	9.91	10.12	11.44	2.07	2.07	2.07
O_2	5.20	6.87	7.54	2.25	2.30	2.29
F_2	1.65	2.69	3.32	2.68	2.65	2.63

tional. Without spherical averaging, our results¹⁹ are closer to the non-self-consistent results of Becke.¹⁸

D. Bond lengths

The theoretical bond lengths, R_e , are also shown in Table IV. The calculated R_e were already quite good with local functionals. The F_2 bond length is slightly better using the nonlocal functional, but otherwise there is little difference.

IV. SUMMARY

Fully self-consistent calculations show that the LM nonlocal functional improves upon the LSDA in describing the depth of dissociation curves of N_2 , F_2 , and O_2 .

With the exception of Li_2 , nonlocality also slightly improves the agreement between calculated and experimental vibrational frequencies and bond length. Within the accuracy quoted in Table III, the N_2 binding energy was not affected by self-consistency in the nonlocal potential, or by altering f between reasonable limits. The means of suppressing the nonlocal potential does slightly affect the binding energies.

ACKNOWLEDGMENT

Research was sponsored in part by the Division of Materials Sciences, U.S. Department of Energy, under Contract No. DE-AC05-84OR21400 with Martin Marietta Energy Systems, Inc.

¹P. Hohenberg and W. Kohn, Phys. Rev. **136**, B864 (1964).

²W. Kohn and L. J. Sham, Phys. Rev. **140**, A1133 (1965).

³Several examples of LDA applications may be found in *Local Density Approximations in Quantum Chemistry and Solid State Physics*, edited by J. P. Dahl and J. Avery (Plenum, New York, 1984).

⁴U. von Barth and L. Hedin, J. Phys. C **5**, 1629 (1972).

⁵S. H. Vosko, L. Wilk, and M. Nusair, Can. J. Phys. **58**, 1200 (1980).

⁶(a) D. C. Langreth and J. P. Perdew, Solid State Commun. **17**, 1425 (1975); (b) Phys. Rev. B **15**, 2884 (1977); (c) Solid State Commun. **31**, 567 (1979); (d) Phys. Rev. B **21**, 5469 (1980).

⁷D. C. Langreth and M. J. Mehl, Phys. Rev. B **28**, 1809 (1983).

⁸(a) C. D. Hu and D. C. Langreth, Phys. Scr. **32**, 391 (1985); (b) Phys. Rev. B **33**, 943 (1986).

⁹R. G. Parr, Annu. Rev. Phys. Chem. **34**, 631 (1983).

¹⁰G. S. Painter and F. W. Averill, Phys. Rev. B **28**, 5536 (1983).

¹¹The molecular-orbital basis set was derived from atomic basis

sets of F. B. Duijneveldt, IBM Research Report No. RJ-945, 1971 (unpublished).

¹²(a) For N_2 , A. Lofthus and P. H. Krupenie, J. Phys. Chem. Ref. Data **6**, 113 (1977); (b) for Li_2 , P. H. Krupenie, E. A. Mason, and J. T. Vanderslice, J. Chem. Phys. **39**, 2399 (1963); (c) for O_2 , J. T. Vanderslice, E. A. Mason, and W. G. Maisch, *ibid.* **32**, 515 (1960).

¹³M. R. Pederson, R. A. Heaton, and C. C. Lin, J. Chem. Phys. **80**, 1972 (1984).

¹⁴H. M. Hulburt and J. O. Hirschfelder, J. Chem. Phys. **9**, 61 (1941).

¹⁵K. P. Huber and G. L. Herzberg, *Molecular Spectra and Molecular Structure. IV Constants of Diatomic Molecules* (Van Nostrand/Reinhold, New York, 1979).

¹⁶G. S. Painter and F. W. Averill, Phys. Rev. B **26**, 1781 (1982).

¹⁷J. G. Harrison, J. Chem. Phys. **78**, 4562 (1983).

¹⁸A. D. Becke, J. Chem. Phys. **84**, 4524 (1986).

¹⁹F. W. Kutzler and G. S. Painter, Phys. Rev. Lett. **59**, 1285 (1987).